CFD Modeling of Three-phase Bubble Column: 2. Effect of Design Parameters

K. L. Wasewar,* M. Anil, and V. K. Agarwal
Chemical Engineering Department, Indian Institute of Technology (IIT),
Roorkee – 247667, Uttarakhand, INDIA

The effect of design parameters on the flow pattern in a three-phase bubble column by means of Computational Fluid Dynamics (CFD) has been studied. The simulations were performed for air-water-glass beads in a bubble column of $H = 0.6$ m, $D = 0.1$ m and $d_s = 0.05$ m to study the flow pattern. Eulerian–Eulerian three-phase simulations with k-ε turbulence for liquid phase were carried out using the commercial flow simulation software CFX-5.6, with a focus on characterizing the dynamics properties of gas liquid solid flows. The model has been validated using available experimental data and is in good agreement. Effect of design parameters such as: H/D ratio, sparger diameter, taperness on the flow pattern has been studied. The results presented are useful for understanding the dynamics of gas liquid solid flows in bubble column, and provide a basis for further development of CFD model for three-phase systems.

Key words:
CFD, bubble column, three-phase reactor, design parameters

Introduction

The bubble column (BC) or slurry bubble column (SBC) reactor has emerged as one of the most promising devices in chemical, biochemical and environmental engineering operations because of its simple construction, isothermal conditions, high heat and mass transfer rates, and *on-line* catalyst addition and withdrawal. In bubble column slurry reactors, a gas is dispersed through a deep pool of liquid containing suspended solid particles. In these reactors, the momentum is transferred to the liquid phase and solid phase by the movement of the gas bubbles. Bubble column reactors have a wide range of applications such as absorption, catalytic slurry reactions, bioreactions, coal liquefications etc. Bubble (slurry) reactors are used extensively to carry out a variety of gas liquid and gas liquid solid reactions. Classic examples are carbonation of lime slurry, chlorination of paper stock, hydrogenation of vegetable oils, aeration of fermentation broths as in the production of penicillin, production of citric acid from sugar by action of microorganisms, and aeration of activated sludge for biological oxidation, etc. Bubble columns are preferred over other multiphase reactors because less maintenance is necessary due to the absence of moving parts, higher values of effective interfacial areas and overall mass transfer coefficients, higher heat transfer rates per unit volume of the reactors, solids can be handled without erosion or plugging problems, less floor space is occupied, and bubble column reactors are less expensive and slow reactions can be carried out due to high liquid residence time.

Computational Fluid Dynamics (CFD) is the science of predicting fluid flow, heat transfer, mass transfer, chemical reactions, and related phenomena by solving the mathematical equations that govern these processes using a numerical algorithm (that is, on a computer). The results of CFD analyses are relevant engineering data used in conceptual studies of new designs, detailed product development, troubleshooting, and redesign. CFD is gaining importance in general process applications. CFD approaches use numerical techniques for solving the Navier-Stokes equations for given flow geometry and boundary conditions thereby implementing models for flow aspects like turbulence or heat and mass transfer as relevant for the specific modeling task. CFD has been an important tool in air and space industry or vehicle design for a long time where it has largely replaced time-consuming and expensive wind tunnel experiments. Yet, while in these applications single-phase flows are prevailing, modeling applications in chemical and biochemical reactors in most cases include multiphase flows the modeling and numerical treatment of which introduce additional challenges. Therefore, multiphase CFD applications have gained broad attention only over the last decade since increasing computational power available has enabled computations previously considered infeasible. Still, most literature reports are limited to two-phase flows, and especially gas-liquid CFD projects often

* Corresponding author; E-mail: k_wasewar@rediffmail.com,
klw73fch@iitr.ernet.in
Phone: +91-1332-285347; Fax: +91-1332-276535

deal only with very low dispersed phase holdups. In effect, this means that multiphase CFD is still far from being a general tool for the practitioner even if recent advances in computational power available in desktop PCs do enable first steps in this direction.

A lot of literature is available on the bubble column. It is evident from the available literature mentioned in Anil[1] and previous paper, Anil *et al.*,[2] that the flow patterns in the bubble column and flow parameters are important for overall column performance. Hence, it is essential to understand the hydrodynamics of the bubble column and effect of various design and process parameters on it. In spite of increasing computational power available for the multiphase CFD application, still, most literature reports are limited to two-phase flows, and especially gas-liquid CFD projects that often deal only with very low dispersed phase holdups. In this paper, the flow pattern in a bubble column using Computational Fluid Dynamics (CFD) based software CFX-5.6 has been studied to assess the effects of superficial gas velocity, solid loading, particle diameter, *H/D* ratio, sparger diameter, taperness on flow pattern behavior and flow quantities in the bubble column.

Mathematical modeling

In multiphase CFD, two main approaches are present. They are classified based on how the dispersed phase (particles, droplets or bubbles) is treated. They are the Eulerian–Eulerian approach and Eulerian–Lagrangian approach.

For the CFD calculations performed as part of this project, the Eulerian–Eulerian approach has been chosen because of its obvious computational advantages at high dispersed phase contents: While the Eulerian–Lagrangian approach suffers from high demands on computational power; this renders them rather unsuitable for the computation of multiphase flows in real process applications where dispersed phase holdups are usually high. Therefore, the Euler-Euler or multi-fluid approach was implemented which allows for the computation of three-phase flow fields even with high solid and gas holdups at reasonable computational expense.

Hydrodynamic model

Assumptions

The following assumptions were made for hydrodynamic modeling of bubble column:

– 3D, transient as well as steady state.

– Isothermal flow conditions, therefore no energy equations.

– Mass transfer and chemical reactions were neglected.

– Buoyancy effect was included in order to correctly model bubble rise.

– Liquid phase turbulence was modeled using the *k-ε* model; the dispersed phases were considered laminar.

– The system of equations was solved using a finite-volume scheme.

– Momentum transfer between the liquid and the dispersed phases was modeled using the appropriate drag laws for the respective flow regime.

– Momentum transfer between the dispersed phases were neglected.

– Bubbles were assumed as rigid spheres having a constant diameter.

Conservation of mass: continuity equation

The continuity equation describes the mass flux into and out of a control volume. The continuity equations for continuous as well as dispersed phase are as follows:

$$\frac{\partial(\varepsilon_\alpha \rho_\alpha)}{\partial t} + \nabla(\varepsilon_\alpha \rho_\alpha v_\alpha) = 0 \tag{1}$$

Where $\alpha = 1, 2, 3$
ε_α is the volume fraction of phase α, and

$$\sum_\alpha \varepsilon_\alpha = 1 \tag{2}$$

Conservation of momentum: equation of motion

In multiphase formulation, momentum balances look slightly different for continuous and dispersed phases. The momentum balance for the continuous phase becomes in the most general formulation:

$$\frac{\partial(\varepsilon_\alpha \rho_\alpha v_\alpha)}{\partial t} + \nabla(\varepsilon_\alpha \rho_\alpha v_\alpha v_\alpha) = -\varepsilon_\alpha \nabla p_\alpha +$$
$$+ \nabla(\varepsilon_\alpha \mu_\alpha (\nabla v_\alpha + (\nabla v_\alpha)^T)) + \varepsilon_\alpha \rho_\alpha g + M_\alpha \tag{3}$$

Momentum exchange between continuous and dispersed phase i.e. liquid-gas and liquid-solid is:

$$M_\alpha = \sum_{\beta=1}^{N_P} c_{\alpha,\beta}(v_\beta - v_\alpha) \tag{4}$$

where,

$$c_{\alpha,\beta} = \frac{3}{4} \frac{C_D}{d_P} \varepsilon_\beta \rho_\beta |v_\beta - v_\alpha| \tag{5}$$

Momentum balance for the dispersed phase is:

$$\frac{\partial(\varepsilon_\beta \rho_\beta v_\beta)}{\partial t} + \nabla(\varepsilon_\beta \rho_\beta v_\beta v_\beta) = -\varepsilon_\beta \nabla p_\beta + \\ + \nabla(\varepsilon_\beta \mu_\beta (\nabla v_\beta + (\nabla v_\beta)^T)) + \varepsilon_\beta \rho_\beta g + M_\beta \tag{6}$$

Momentum exchange between continuous and dispersed phase i.e. liquid-gas for gas phase and liquid-solid for solid phase is:

$$M_\beta = c_{\alpha,\beta}(v_\beta - v_\alpha) \tag{7}$$

where

$$c_{\alpha,\beta} = \frac{3}{4} \frac{C_D}{d_P} \varepsilon_\beta \rho_\beta |u_\beta - u_\alpha| \tag{8}$$

For liquid-gas,

$$C_D = 0.44 \qquad Re > 1000 \tag{9}$$

and for liquid-solid,

$$C_D = \frac{24}{Re}(1 + 0.15 Re^{0.687}) \qquad Re \le 1000 \tag{10}$$

Turbulence modeling

Turbulence modeling is of crucial importance for the correct description of multiphase flows in CFD modeling. In this study, one of the most prominent turbulence models, standard *k-ε* model was considered which has been implemented in most general purpose CFD codes and is considered the industry standard model. It has proven to be stable and numerically robust and has a well-established regime of predictive capability. For general-purpose simulations, the *k-ε* model offers a good compromise in terms of accuracy and robustness.

Since in the computations carried out here the liquid phase is continuous, the conservation equation for the liquid turbulent kinetic energy *k* may be written as follows:

$$\frac{\partial}{\partial t}(\varepsilon_l \rho_l k) + \frac{\partial}{\partial x_i}(\varepsilon_l \rho_l u_{l,i} k) - \\ - \frac{\partial}{\partial x_i}\left(\varepsilon_l\left(\mu_{l,lam} + \frac{\mu_{l,turb}}{\sigma_k}\right)\frac{\partial k}{\partial x_i}\right) = \varepsilon_l(G - \rho_l \varepsilon) + S_{l,k} \tag{11}$$

Here, *G* is a turbulence production term and $S_{l,k}$ is a source term; both of these may be used to e.g. implement turbulence effects of bubbles or particles but are not considered here and thus set to zero.

The conservation equation for the liquid turbulent dissipation *ε* is:

$$\frac{\partial}{\partial t}(\varepsilon_l \rho_l \varepsilon) + \frac{\partial}{\partial x_i}(\varepsilon_l \rho_l u_{l,i} \varepsilon) - \\ - \frac{\partial}{\partial x_i}\left(\varepsilon_l\left(\mu_{l,lam} + \frac{\mu_{l,turb}}{\sigma_\varepsilon}\right)\frac{\partial \varepsilon}{\partial x_i}\right) = \varepsilon_l(C_{\varepsilon_1}G - C_{\varepsilon_2}\rho_l \varepsilon) + S_{l,\varepsilon} \tag{12}$$

The source term $S_{l,\varepsilon}$ is set to zero as with $S_{l,k}$.

The effective liquid dynamic viscosity is combined for the turbulent case from a laminar and a turbulent part:

$$\mu_\alpha = \mu_{\alpha,lam} + \frac{\mu_{\alpha,turb}}{\sigma_k} \tag{13}$$

Where the turbulent viscosity $\mu_{\alpha,turb}$ is computed from:

$$\mu_{\alpha,turb} = C_\mu \rho_l \frac{k^2}{\varepsilon} \tag{14}$$

In effect, this means that with the *k-ε* model, three additional unknowns (*k*, *ε* and $\mu_{\alpha,turb}$) and three equations (two partial differential equations, one algebraic equation) have been introduced into the calculation yielding a closed model.

Initial and boundary conditions

In order to obtain a well-posed system of equations, reasonable boundary conditions for the computational domain have to be implemented.

– With the three-dimensional calculations carried out in this project, no symmetry conditions as with 2D models were needed.

– At the walls, a no-slip boundary condition was implemented for liquid phase and free slip for gas and solid phase.

– For liquid and solid phase, reactor bottom and top were considered as walls, while the gaseous phase was allowed to enter through a patch at the reactor bottom the shape of which depended on the sparger geometry.

– The sparger cannot be modeled with all its holes but has to be modeled as a flat surface where a constant normal gas velocity and gas holdup can be prescribed. In reality, however, the local gas velocity at the small sparger holes is substantially higher leading to a better fluidization of solid particles than in the model case.

– At the reactor top, a special degassing boundary was set up where air and excess liquid or solid were allowed to leave the reactor ("overflow").

– Transient calculations started from assuming fully fluidized state with an integral gas holdup of $\psi = 5\%$ and integral solid loading according to the desired value in the calculation (i. e. $\psi = 0$, 5 or 10 %).

Results and discussion

In this work, the flow in three-phase bubble column was modeled using the Eulerian-Eulerian model incorporated in CFX-5.6. The details of the standard geometry and three-phase system used to study the flow pattern are used as earlier.[2] Unstructured tetrahedral mesh was generated for bubble column. For CFD simulations $10 \times 20 \times 60$ grid was used. The details of the geometry, system and the range of design variables used for the parametric sensitivity studies are given in Table 1, Table 2, and Table 3 respectively.

T a b l e 1 – *The standard reactor geometry used to study the flow pattern in bubble column*

bubble column height, H	0.6 m
bubble column diameter, D	0.1 m
plate sparger diameter, d_s	0.05 m
superficial gas velocity, u_g	0.6 m s⁻¹
solid loading, ψ	10 %
average mesh width/grid cell edge length	1 cm
reference pressure, p	1 bar

T a b l e 2 – *Three-phases in the bubble column system*

Material	Morphology	Diameter d/mm	Density ρ/kg m⁻³
air	dispersed fluid	5	1.185
water	continuous fluid	—	997.0
glass beads	dispersed solid	1	1200

T a b l e 3 – *Range of design variable used*

H/D ratio	2, 4, 6, 8, 10, 12, 14
sparger diameter, d_s/cm	2, 4, 5, 6, 8
taperness (outlet dia./inlet dia.)	1, 1.2, 1.4, 1.6, 1.8, 2

Model validation

The model was validated using the experimental data of Michele and Hempel.[3] A comparison of computed and measured integral gas holdups for bubble column of $H = 6$ m, $D = 0.63$ m, $d_s = 0.057$ m and solid loading $\psi = 10$ % were carried out.[2] Details are given in the earlier paper of Anil *et al.*[2]

For the lower range of superficial gas velocity ($u_g <$ 0.07 m s⁻¹), CFD model results are up to 20 % underpredicted. For higher superficial gas velocity ($u_g > 0.07$ m s⁻¹), model results are in good agreement with experimental results. Agreement between measurement and modeling results with respect to integral gas holdup was quite good.

The model was capable of capturing the right order of magnitude of gas holdup and general dependency of gas holdup on superficial gas velocity, it cannot account for the different flow regimes observed in the measurements. While measurement data clearly show the division line between homogeneous and heterogeneous flow regime at a superficial gas velocity of approximately 0.03 m s⁻¹ (marked by a distinct decrease of the graph's slope), the modeling calculations yield a slightly linear relation between superficial gas velocity and integral gas holdup for the whole range under consideration, where agreement with the experimental data is best at very low and very high superficial gas velocities. This could be due to non-inclusion of Magnus force and effect of surface tension. Thus, further model improvements are needed to deal primarily with correctly covering the different flow regimes, e.g. by implementing models for bubble size distribution depending on the superficial gas velocity. A similar type of limitation was observed in computation of local liquid flow velocities. Similar results were obtained by Michele and Hempel.[7]

Effect of *H/D* ratio

The height to diameter ratio (H/D) has a considerable effect on the performance of the bubble column. The effect of H/D ratio on hydrodynamic (velocity and holdup of gas, liquid, and solid) of bubble column has been systematically investigated and is given in Figs. 1 to 6. It has been observed from Figs. 1, 2, 3 that at low H/D ratios velocities of all the phase are high and remain constant throughout the axial length this is due to jetting at low H/D ratio. Whereas, at high H/D ratios there is a gradual decrease in velocity along the axial length. With an increase in the H/D from 2 to 14, a significant decrease in the magnitude of the liquid, gas and solid velocity occurs. An increase in height to diameter ratio (H/D) from 2 to 14 causes a decrease in the maximum upward velocity by about 3 times. The maximum downward velocity also decreased by about 3 times.

From Fig. 4, it can be observed that the gas holdup at low H/D ratios is high and almost constant along the axial length. For high H/D ratios, gas holdup decreases gradually and is then constant along the remaining axial length of the column. In case of low H/D ratio, the rate of coalescence of
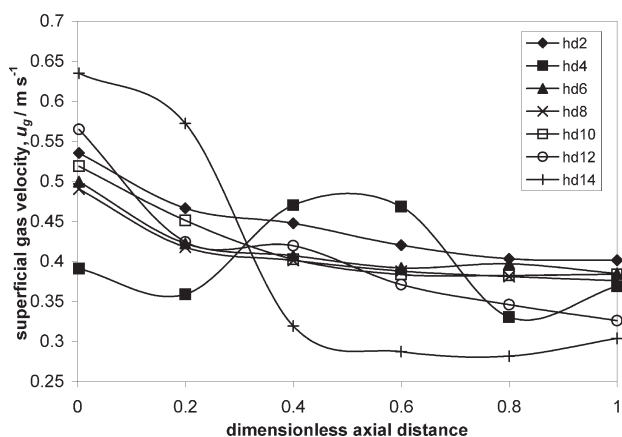
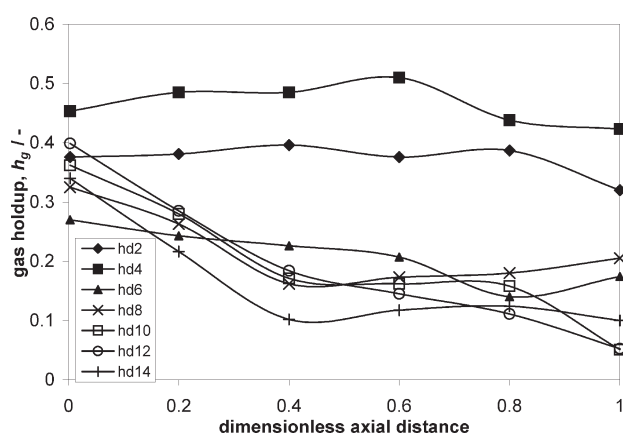F i g . 1 – *Effect of H/D ratio on superficial gas velocity*
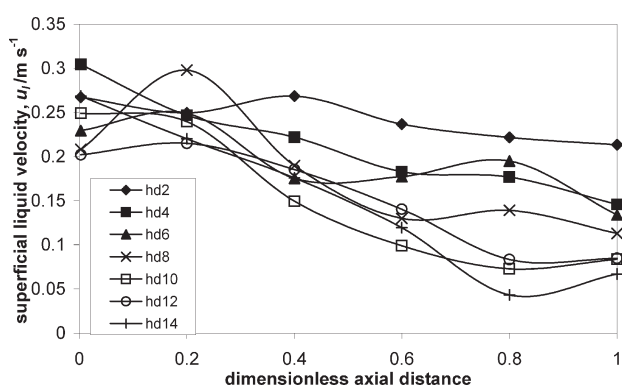

F i g . 2 – *Effect of H/D ratio on superficial liquid velocity*

F i g . 3 – *Effect of H/D ratio on superficial solid velocity*

F i g . 4 – *Effect of H/D ratio on gas holdup*

F i g . 5 – *Effect of H/D ratio on liquid holdup*

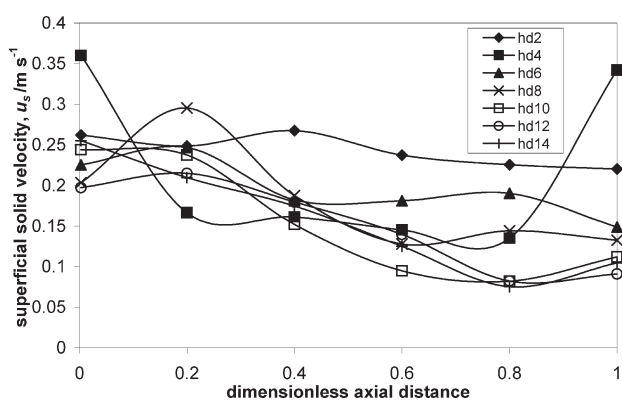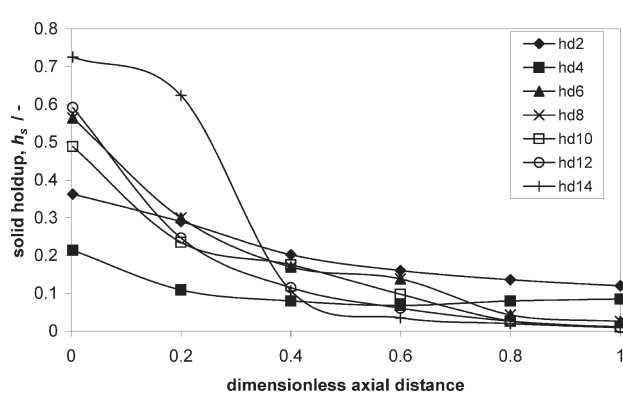

F i g . 6 – *Effect of H/D ratio on solid holdup*

bubbles is almost constant at the height of the column, hence an almost constant gas holdup was observed along the axial length. In case of high *H/D,* coalescence rate of bubbles decreased and then became constant, hence, gas holdup decreases gradually and then becomes constant along the remaining axial length of the column.

The liquid holdup (Fig. 5) is very low for low *H/D* ratio but for other *H/D* ratios it increases along the axial length. For low *H/D* ratio, the solid holdup as shown in Fig. 6, remains almost constant throughout the axial length but for other *H/D* ratios

it decreases along the axial length, while for high *H/D* ratios the solid holdup is almost zero at upper section meaning that the solid particle does not reach the top of the bubble column. The highest solid holdup can be found immediately above the sparger with the maximum shifting to the center with increasing height. At low *H/D* ratios, the gas velocities are enough to bring the solid particles at the top edge of the column as compared to high *H/D* ratio. The decrease in solid holdup is less in case of low *H/D* (almost constant) as compared to high *H/D* ratio.

Effect of sparger diameter

The effect of sparger diameter on velocity and holdup of gas, liquid, and solid in three-phase bubble column is shown in Figs. 7 to 12. The effect of sparger diameter is not so significant on superficial gas velocity, as is shown in Fig. 7, but still for lower sparger diameter the gas superficial velocity is low, and for higher sparger diameter the gas superficial velocity is high. From Figs. 8 and 9, it is observed that the profiles of superficial both liquid and solid velocities are almost similar as seen for particle size. This is because the solid particle was

created in thermodynamic state as a liquid with morphology as a dispersed solid, which is why its behavior is similar to that of liquid.

It is obvious from Fig. 10 that, as the sparger diameter increased, the gas holdup inside the bubble column also increased, because more amount of gas is passed into the bubble column. For liquid holdup (Fig. 11), the effect of sparger diameter is opposite to that observed for gas holdup i.e. as the sparger diameter is increased the liquid holdup decreased inside the bubble column. For solid holdup, as shown in Fig. 12, it can be observed that for low sparger diameter the solid particle reached only up
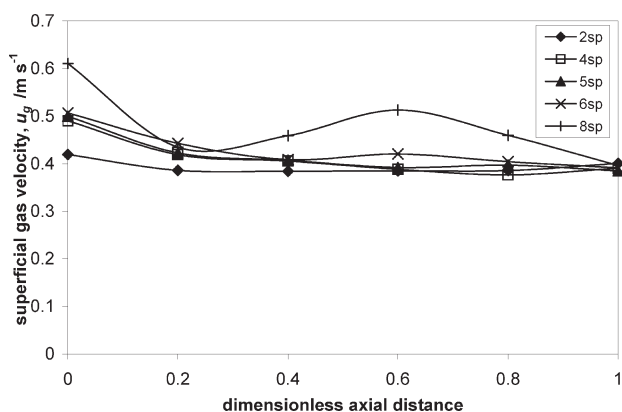

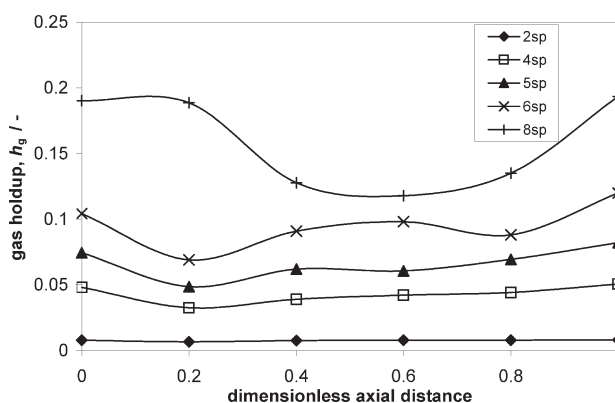F i g . 7 – *Effect of sparger diameter on superficial gas velocity*

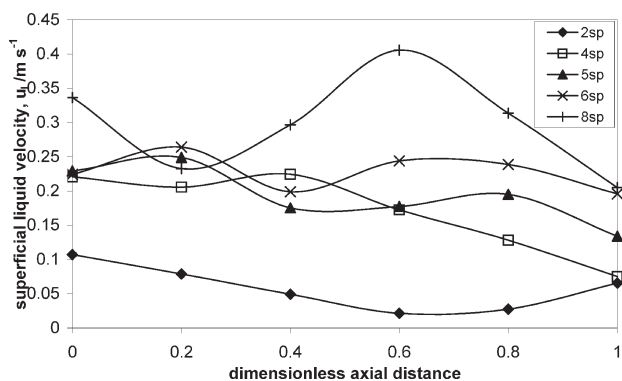F i g . 8 – *Effect of sparger diameter on superficial liquid velocity*

F i g . 9 – *Effect of sparger diameter on superficial solid velocity*

F i g . 1 0 – *Effect of sparger diameter on gas holdup*
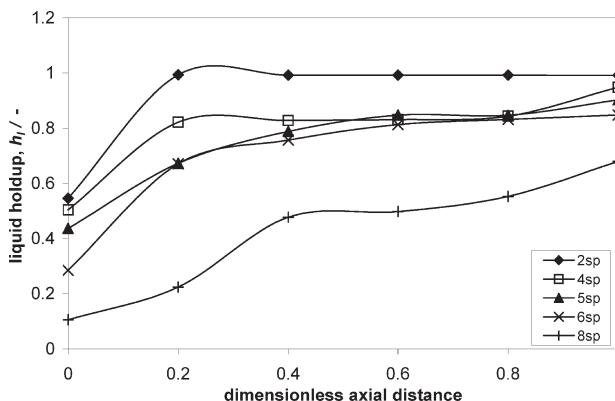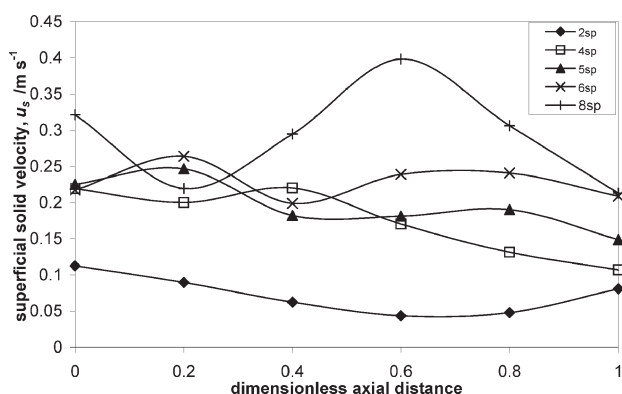

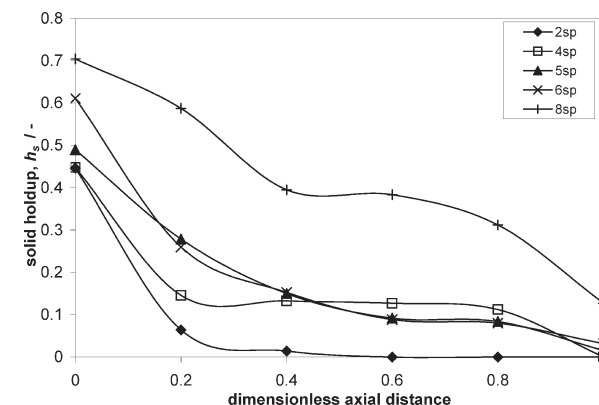F i g . 1 1 – *Effect of sparger diameter on liquid holdup*

F i g . 1 2 – *Effect of sparger diameter on solid holdup*

to center of the bubble column, whereas for bubble column with larger sparger diameter the solid particle reaches the top of the column. For low sparger diameter, the solid particle dispersed radially also. Therefore it will not only reach the centre but also the radial zone. This is due to more kinetic energy for low sparger diameter. When the sparger diameter is smaller, the area on which bubbles are formed is smaller also, resulting in easier coalescence between the bubbles on the sparger area. Consequently, large bubbles, due to the coalescence of the under-formation bubble, start to form at lower gas flow rates when the sparger of smaller diameter is

employed resulting in the earlier transition to the heterogeneous regime. The sparger diameter does not greatly influence gas holdup as long as the pseudo-homogeneous regime exists. However, when the heterogeneous regime is established, for the column with smaller sparger diameter, the gas holdup is lower compared to a column with larger sparger diameter, for the same gas flow rate.

Effect of taperness

Effect of taperness on velocity and holdup of gas, liquid, and solid in three-phase bubble column is shown in Figs. 13 to 18. It has been observed
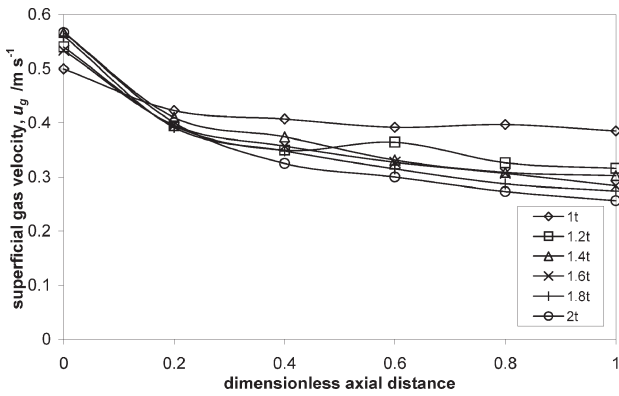

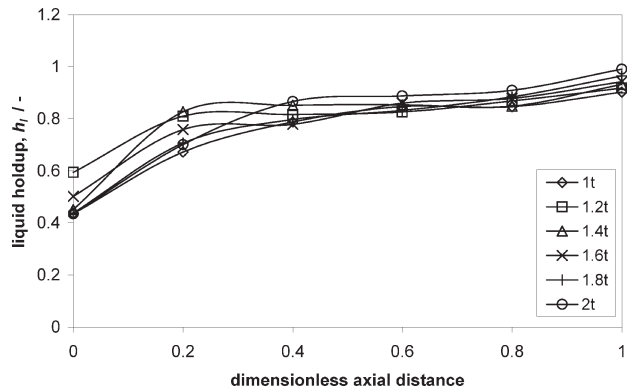F i g . 1 3 – *Effect of taperness on superficial gas velocity*
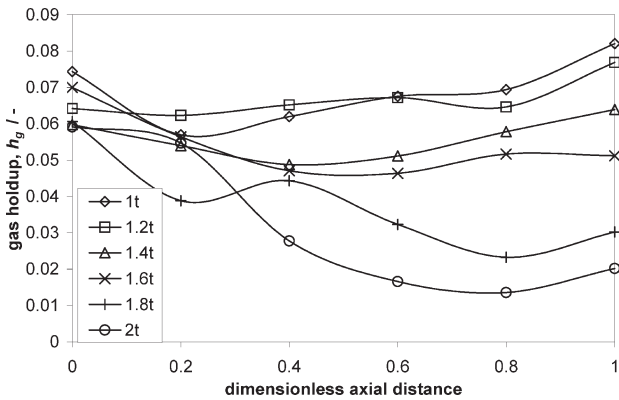

F i g . 1 6 – *Effect of taperness on liquid holdup*

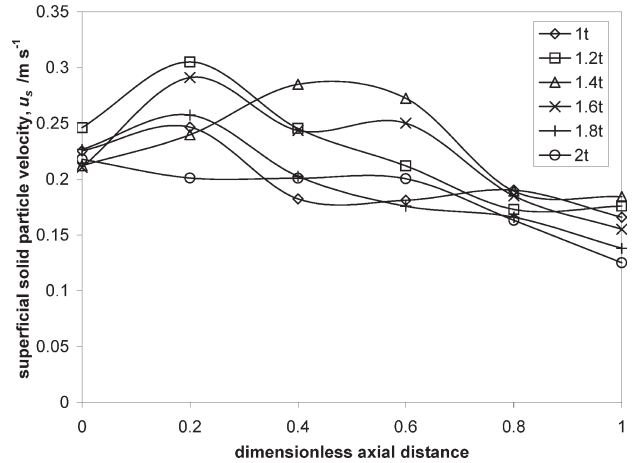F i g . 1 4 – *Effect of taperness on gas holdup*

F i g . 1 7 – *Effect of taperness on superficial solid velocity*
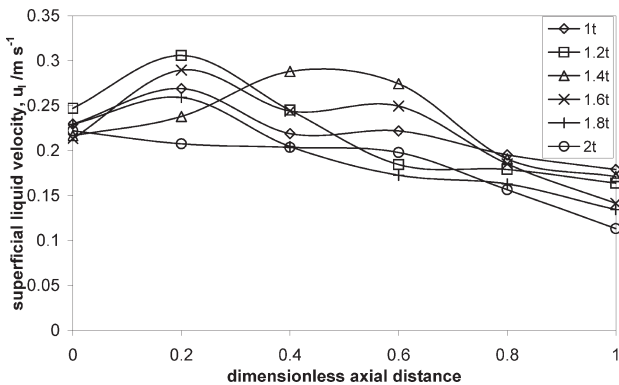

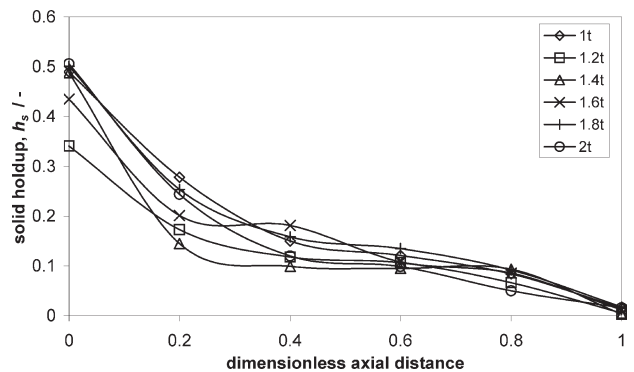F i g . 1 5 – *Effect of taperness on superficial liquid velocity*

F i g . 1 8 – *Effect of taperness on solid holdup*

from Fig. 13 that the gas velocity progressively decreases in axial direction but the decrease is more prominent in case of taper bubble column compared to cylindrical bubble column i.e. as the taperness increases the gas velocity decreases. Similarly, for the case of gas holdup (Fig. 14) in cylindrical bubble column, gas holdup increases in axial direction, whereas for tapered bubble column the gas holdup progressively decreases in axial direction. The gas holdups progressively decrease in axial direction due to the reduction of superficial gas velocity from the bottom to the top. However, the gradient of axial gas holdup gradually increases when taperness becomes high. This is significant in the case of higher taperness of the column. In this case, bubble rise vertically without remarkable interaction and their sizes depend on the distributor design and on the physical property of the liquid in the bubbly regime while bubbles tend to coalesce or break up in the transitional or turbulent regime.

Not much effect of taperness is seen on liquid velocity (Fig. 15) but for liquid holdup (Fig. 16) there is an increase in liquid holdup in axial direction for tapered bubble column. Liquid holdup is slightly increased in tapered column as compared to cylindrical bubble column. It can be observed from Fig. 17, that the solid particle velocity is low for taper bubble column compared to cylindrical bubble column. For solid holdup as shown in Fig. 18, there is an exponential decrease in axial direction. The reason for all the above axial profiles is the increase in diameter of taper bubble column in axial direction. The solid holdup at the top of the column is almost the same in all columns.

Conclusion

This paper is a continuation of our previous paper Anil *et al.*[2] A CFD model for three-phase bubble column has been developed to study the effect of various design parameters on the hydrodynamics in bubble column. The effect of *H/D* ratio, sparger diameter, column taperness on superficial gas velocity and gas holdup, liquid and solid have been studied using CFD software CFX-5. The model results have been compared with the experimental results, and prove to be in good agreement.

The *H/D* ratio, sparger diameter and taperness have marked influence on distribution of the solid particle. For almost all the ranges of variables studied, the liquid phase holdup or solid phase holdup at the lower region differs significantly from the corresponding holdup at the upper region of bubble column, indicating that the amount of dispersion in solid phase is not large.

Nomenclature

C_D – drag coefficient, s^{-1}

d_p – diameter of single particle, m

d_s – sparger diameter, m

D – column diameter, m

g – gravitational acceleration, $m^2\ s^{-1}$

H – column height, m

h – holdup

k – turbulence kinetic energy, $m^2\ s^{-2}$

M – momentum exchange term, $kg\ m^{-2}\ s^{-2}$

p – pressure, Pa

Re – Reynolds number

t – time, s

u – superficial fluid phase velocity, $m\ s^{-1}$

$(v_\alpha - v_\beta)$ – relative velocity between two phases, $m\ s^{-1}$

v – velocity, $m\ s^{-1}$

Greek Letters

ρ – phase density, $kg\ m^{-3}$

σ – interfacial tension, $N\ m^{-1}$

υ – kinematic viscosity, $m^2\ s^{-1}$

ε – turbulence eddy dissipation, $m^2\ s^{-3}$

ε_α – holdup of phase α

μ – dynamic viscosity, $kg\ m^{-1}s^{-1}$

ψ – volume fraction

Subscripts

α – phase

g – gas phase

l – liquid phase

s – solid phase

1 – gas phase

2 – liquid phase

3 – solid phase

References

1. *Anil, K.,* M. Tech. Dissertation, IIT Roorkee, INDIA 2004.
2. *Anil, K., Agarwal, V. K., Alam, S., Wasewar, K. L.,* Chem. Biochem. Eng. Q. **3** (2007) 197.
3. *Michele, V., Hempel, D. C.,* Chem. Eng. Sci. **57** (2002) 1899.